# An Adaptable Lateral Resolution Acoustic Beamforming for the Internet of Bio-Nano Things in the Brain

Hanna Firew and Michael Taynnan Barros, *Member, IEEE,*

*Abstract*—The Internet of Bio-Nano Things in the Brain are minimally invasive untethered links between the brain tissue and silicon platforms. Even though these interfaces have been envisioned for many biomedical applications, it is unclear how the ultimate technology will support spatially distributed networks. In this paper, we address the distributed power allocation through adaptable beamforming by varying the acoustic beam lateral resolution. Our results show improvements in average power transfer efficiency for sparser beams compared to narrower ones for a randomly placed network of implantable devices with 15 nodes within a 4mm$^2$ space in the neocortex.

*Index Terms*—Neural Interfaces, Wireless Network, Ultrasound beamforming, Neural dust, Network Adaptation

## I. INTRODUCTION

Neurodegenerative diseases are a burden to the ageing society as the biggest challenge is to provide early detection and treatment for chronic diseases without traumatic intervention. While most treatment approaches focus on chemicals or surgery, the emerging area of electroceuticals provides approaches based on the Internet of Bio-Nano Things focusing on stimulation and sensing of brain tissue [1]–[3]. Current deep brain stimulation (DBS) solutions are bulky - they include invasive probes and leads implanted in the patient's brain to allow current injection and neural stimulation actions [4].

Wireless brain interfaces have been introduced recently with the potential to overcome these limitations and challenges of existing invasive solutions by providing completely untethered solutions. Stimulation current is provided by either a passive wireless current injection to neurons or an active one, where a device converts a wirelessly radiated energy to a current with adequate frequency and impedance matching so that stimulation is achieved [5], [6]. However, to do so, a network of multiple implanted devices would provide extended capabilities for controlling patterns and codes of populations of neurons, which would lead to more effective treatment based on stimulation. The network of wireless neural interfaces has only been initially hinted at in the literature for infrared media [7]. This technology not only supports directional communication with multiple devices based on ultrasound signals but supports half-duplex communications and networks services such as addressing, multi-hopping or routing for example [8]. To achieve that, we must develop the building blocks such as signal processing and protocols that manage computing and energy resources in the wireless neural interfaces.

Current literature reports mostly on the usage of straight beams with mostly high acoustic frequency (>5MHz) and

H. Firew is with the Faculty of Medicine and Health Technology, Tampere University, Finland.

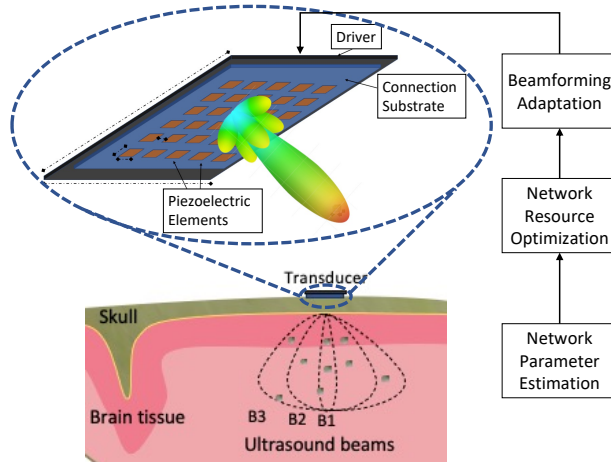M. Barros is with the School of Computer Science and Electronic Engineering, University of Essex, UK.

Fig. 1. Sketch of intended adaptable setup for networked wireless implantable neural interfaces controlled and powered by ultrasound beam.

static lateral resolution. There are also reliable examples transducer configurations that provides enough power to achieve great efficiency in single devices in animal models, but not in multiple networked devices in both numerical or non-biological experimental platforms. The main question now that is put forward is what beamforming techniques should emerge and that is what our contributions are focused.

Inspired by techniques of beam manipulation in ultrasound medical imaging, we propose an adaptable beamforming technique that allows the selection of devices based on the lateral resolution of the acoustic beam. Lateral resolution is defined as the level of acoustic pressure variation from the focal point in the horizontal axis. It is controlled by the acoustic carrier frequency, and ultimately expands and contracts the beam over the network space. This approach presents not only the ability to coordinate what devices will be active but allows the possibility of addressing devices based on their geographic position in the Brain tissue. We evaluate our method by combining numerical and simulations based on the Transducer Array Calculation (TAC) platform developed by Kohout et al. [9]. We were able to accurately define a transducer array set up with revised parameters to control the lateral resolution of the beams. We characterize the effects of lateral resolution-based beamforming by calculating the average received power and average power transfer efficiency when scaling the number of network nodes. Our results show that while lateral resolution indeed achieves selective of the devices, the average efficiency was non-constant throughout the network. This means that devices can operate on different time scales due to the energy harvesting process, which is suitable for asynchronous networks.

## II. ACOUSTIC LATERAL RESOLUTION-BASED BEAMFORMING TECHNIQUE

In medical imaging, the lateral resolution is used to observe the spatial range of the beam to evaluate the diffusion of sound pressure in a certain area surrounding the focal acoustic intensity point. We use this concept to investigate that given the size of the network, we can adapt the lateral resolution of the beam to provide selectivity in the network. We aim to provide the required developed theoretical work to demonstrate the feasibility of our approach. We do not, however, provide utility to such selectivity feature since it can be used for various building blocks for developing a full network solution, including addressing or energy harvesting strategies. In this section, we put forward the necessary models that explain the propagation of an acoustic beam from a transducer array composed of squared sources, the lateral resolution-based beamforming as well as the acoustic attenuation losses from skull and tissue.

### A. Acoustic Beam Propagation based on Transducer Array of Squared Elements

Acoustic beam propagation was modelled and evaluated through a directive wave pattern description based on sound fields generated by squared transducers in far and near fields (see Fig. 1). We consider a transducer array with $N$ elements with an area of $\Delta A = \Delta h \Delta w$ as $\Delta h$ and $\Delta w$ are the dimensions of each transducer. The transducer is separated by a constant spacing space that results in simple homogeneous distributions of transducer across the array area. We consider a transducer of piezoelectric material placed in a connective substrate to a driver, that controls the current delivered to each transducer. Even though the circuitry of the driver is not explored in this paper, the proposed lateral resolution-based beamforming requires a new design to deal with protocols and device communications similar to [10], [11], and therefore the present theoretical study is important to capture its feasibility. The pressure of the sound field formed by $N$ transducers will have a total pressure $p_0$ at a point in the field-dependent on the complex surface velocity for each element in the array ($u_n$) and the pressure field generated by each element ($P_n$) as well, defined as

$$p_0 = \frac{j \cdot \rho \cdot c}{\lambda} \sum_{n=1}^{N} u_n \cdot P_n \qquad (1)$$

Ocheltree and Frizzel [9] define $P_n$ as the integration of the spherical wave produced by each element, as done in the conventional surface integral technique, and defined as

$$P_n = \int_{-h/2}^{h/2} \int_{-w/2}^{w/2} \frac{e^{-(\alpha + j \cdot k)r}}{r} dx_0 dy_0 \qquad (2)$$

with $r = \sqrt{z^2 + (x - x_n - x_0)^2 + (y - y_n - y_0)^2}$, where j $= \sqrt{-1}$, $\rho$ is density of medium, $c$ is the phase velocity of the sound wave, $\lambda$ is the wavelength, $k$ is the wave number, $\alpha$ is the attenuation coefficient, $r$ is the distance between the field point and an element area of the sound source piston, $dx_0$ and $dy_0$ are the dimensions of the single element in the transducer array [9]. Note that the intervals [-h/2,h/2] and [-w/2,w/2] represent the area of the transducer array.

### B. Lateral Resolution-based Beamforming

To determine the relationship between the geometry of the beam and its frequency, we investigate the proposed modelling for lateral resolution ($gamma$). Even though our objective differs from that proposed for lateral resolution, the same relationship between frequency and beam shape holds, and there is a wealth of literature that can be analysed and incorporated into the distributed acoustic energy harvesting problems. Since we already have a solution for acoustic propagation based on Eq. (2), the ultrasonic radiation for a single element can be derived proportionally so that there is a direct correlation between frequency and lateral resolution at $r$. As demonstrated by [12], each dimension can be treated independently. Here, we concentrate on reducing $r$ to the $x$ dimension (with $z = y = 0$), and we assume that the focal point of the ultrasonic wave at $r$ obtains the following expression:

$$P_n \propto \text{sinc}\left(\frac{Lx}{\lambda r}\right), \qquad (3)$$

and considering that the resolution is defined as the distance from the peak of the beam to the point zero of the beam, we can solve Eq. (3) considering it equal to zero, thus yielding to $\gamma = \frac{r}{L}$. For a given frequency $f$, and a cost function $c(f)$ we define that there is an associated $\gamma$ that produces a maximisation of this cost function. Such cost function should be related to the objective of the network in terms of performance. In this paper we focus on the network efficiency of the power transfer, which is defined in the next sections.

### C. Transcranial acoustic absorption

The skull is a brain-protective barrier not only for avoiding foreign body contact with it but as well as protecting tissue perturbation through acoustic signals. Acoustic signals dissipate around the skull and, for a scenario of transcranial penetration of acoustic waves, it can become a major challenge. For batteryless devices depending on acoustic energy conversion, means that the skull will cause a major loss of energy that could be harvested. Literature ( [5]) shows that we can quantify such losses using the attenuation coefficient ($\alpha$), which is defined as the relationship between the frequency used for acoustic transmission ($f$) and the relaxed frequency ($f_s$) due to soft matter propagation

$$\alpha = \frac{A \cdot f \cdot f_s}{\lambda \cdot (f^2 + f_s^2)} \qquad (4)$$

where $A$ is a empirical constant. We can assume that the frequency relaxation and $\lambda$ can be estimated also through a new empirical constant ($a$) to simplify the relationship with $\alpha$ and $f$ thus obtaining $\alpha(f) = a \cdot f$.

### III. NETWORKED WIRELESS IMPLANTABLE NEURAL INTERFACES

For the network design, we defined a hierarchical and centralized set-up by having an external primary device (the ultrasound transducer) and implantable secondary devices (the miniaturized implants). The ultrasound transducer is placed 1) outside of the skull on the surface of the skin and 2) at the dura space between the skull and the brain tissue. In both
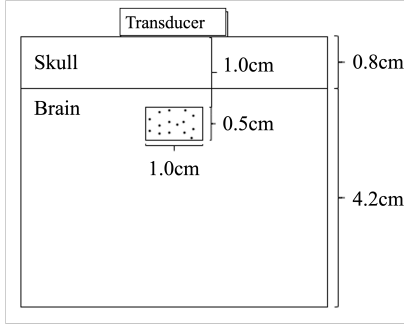
Fig. 2. Illustration of the network structure used in our network response analysis.

cases, the ultrasound beam will travel through different tissue layers before it reaches the devices implanted in the brain (see Fig. 1). The beamforming performance was computed through an algorithm that produces a network response to a determined beam and analysed through received power and the efficiency of the power transfer from the transducer to the implantable device. We describe in the following the device response as well as the network response respectively.

### A. Device response

Efficiency of the power transfer from transducer to the implantable device as percentage is then calculated as:

$$E = \frac{P_{\text{sb}}}{P_{\text{in}}} \cdot 100 \qquad (5)$$

where $Psb$ is power in the skull or in brain and $Pin$ is initial power [5]. Initial power is calculated as $P_{\text{in}} = \frac{p^2}{2\rho c} \cdot A_d$, where $p$ is the initial pressure of the ultrasound wave, $\rho$ is the density of the medium and $c$ is the velocity of the sound wave in the medium and , $A_d$, which is the effective area of the piezoelectric element of the implantable device [13]. In this case, the medium is the skull. Received power behaviour in a point in the field is calculated as:

$$P_{\text{sb}} = \frac{p^2}{2 \cdot \rho \cdot c} \cdot 10^{\frac{-(\alpha f d}{10)}} \cdot A_d, \qquad (6)$$

where this is the intensity of the sound wave in the skull or brain as explained above. $\alpha$ is the attenuation coefficient of the medium, $f$ is the frequency of the sound wave and $d$ is the distance from the transducer to a point in the field.

### B. Network response

A network of wireless brain interfaces analysis objective is to obtain a link between the produced ultrasonic beam from a transducer array so that a collective quantification of received power and power transfer efficiency is obtained. This is not only a spatial problem but an efficiency problem as well. There is a probability of the device being included in the near field of the beams with a tendency of some devices being further away in the far-field. Then as the signal propagates in the brain tissue further devices may need more time to convert the energy necessary to function. We assume that the network of wireless neural interfaces will reside in sub-centimetre area, which may be limited compared to the whole brain's volume, but sufficient to target the scale of a population of neurons. The structure of the network analysis is depicted in Fig. 2 We

consider the placement of a maximum, arbitrarily chosen, 15 neural interfaces in the network area using a random uniform distribution. To obtain the collective quantification of network response to the beamforming, we calculate the average powers and efficiencies from the device response model. We assume that when a device is out of the beam reach, both power and efficiency become zero. We analyse an arbitrary network located in the brain neocortex considering also the average thickness of a human brain's skull. The deepness of the network is about 1.5cm with an average network area of $0.5\text{cm}^2$. The spacing of the network was defined based on the previously obtain beam width analysis from a set of 10x10 transducer elements. The objective of this paper is not to focus on the optimisation of the transducer, since there is a wide variety of existing predefined transducers that are commercially available. Therefore, we kept the network dimensions static throughout our analysis.

## IV. RESULTS

### A. Transcranial Ultrasound Simulations

The presented results in this section were made through the Transcranial Ultrasound Simulations (TAC) proposed in [9]. TAC provides the beams and sound pressure distribution with 2D/3D visualization of beamforming in near and far-fields. The acoustic pressure of the beams differs between a few thousand pascals to megapascals based on 9 different beam shapes. We will show how these changes can dramatically alter the network-wide energy provision, where small scale neural implants are impacted the most.

### B. Analysis of Skull Acoustic Loss

Many works in the literature point out scenarios where the transducers are only placed in the subdural space. We also evaluated the received power behaviour of the beam with or without the skull (see Fig. 4). To mimic in vivo conditions speed of sound in the medium was set to 3500 m/s (average speed of sound in cortical bone [14]) , which is the speed of sound in skull [15]. From the results, we can see that skull causes a barrier that attenuates ultrasound beam at a lot higher rate than brain tissue. In a case in which there is no skull, based on the performed simulations initial pressure would be higher due to the slower speed of sound in the brain. The initial intensity and therefore initial power is higher when there is no skull between the transducer and the brain tissue.

### C. Power and efficiency of a single device

Fig. 3 shows 9 beams produced with sine waves with frequencies from 50 kHz (beam 1) to 100 MHz (beam 9), It was assumed that a single device is placed up to 5 cm away from the transducer array on a straight vertical line below the transducer's central point (see Fig. 2). Power levels of the 9 beams differed from high and sufficient levels of power to too low-level power in the brain. Higher frequency waves (5 MHz or higher) result in higher initial pressure and higher initial power, but will also have a higher attenuation impact. Lower frequency waves can provide enough pressure in brain tissue despite lower initial pressure since it will be less impacted by attenuation. The efficiency of power transfer from the external transducer to the implantable device was calculated for the
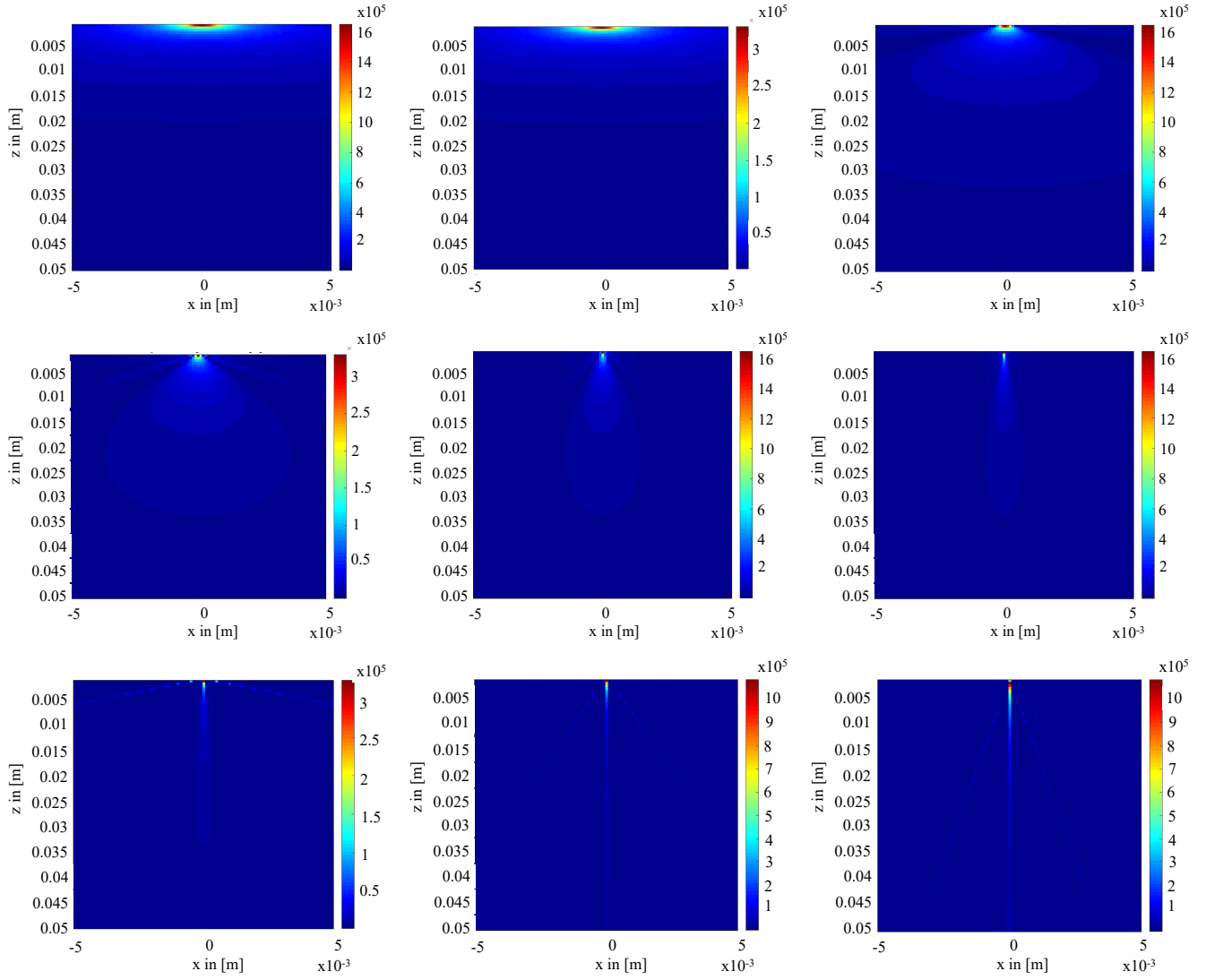
Fig. 3. Beams achieved from simulations with TAC. Frequencies used on simulations: top row from left to right is 50 kHz, 100 kHz and 500 kHz; middle row from left to right is 1 MHz, 2.5 MHz and 5 MHz; bottom row from left to right is 10 MHz, 50 MHz and 100 MHz.

corresponding beams 1-9. Fig. 5 presents average efficiencies in a varying distance between 1cm to 5cm from the transducer across all devices in a network. Efficiency is defined by Eq. (6). The efficiency drastically decreases as the frequency of the sound wave increases exponentially. The beam 1 at 1 MHz decreased nearly 98% to beam 5 at 2/5 MHz.

### D. Power and efficiency of the network

Based on the above-mentioned power results for a single device, three beams (beams 3-5) were chosen for further network calculations to facilitate the impact of widening the beams with beam 3 the widest and beam 5 the most narrow. More complex beamforming techniques may be deployed, however, the paper's goal is to show that even with conventional beamforming techniques, higher efficiency can be achieved. All three beams can provide a possibly sufficient amount of power at least 10 mW [16] and the frequency of waves is commonly used in other studies in the literature. We can see that in the beginning average received power in the brain remains stable for each beam but after an individual
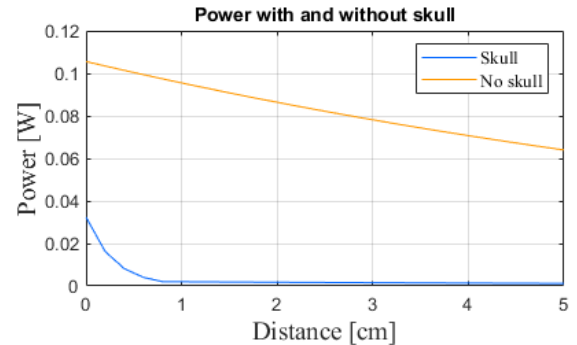


Fig. 4. Power behavior of the beam with single implantable device when skull is present in the scenario.

point, each graph has a drop in the power level, Fig. 6. As the beams widen, it allows a broader coverage of devices is achieved. In the network evaluation of the efficiency, we can see the same behaviour as with the power evaluation (see Fig. 7). As more devices are in the range of the beam with beam
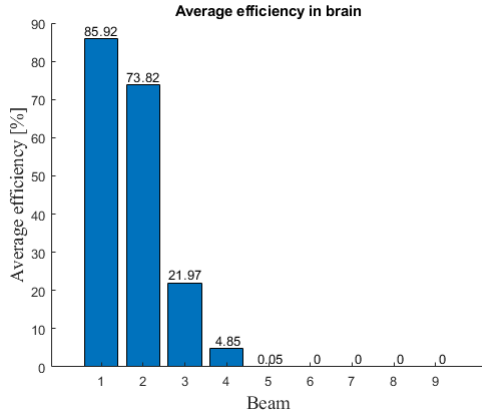
Fig. 5. Average efficiency of power transfer from the transducer to implanted device in brain for single implantable device.
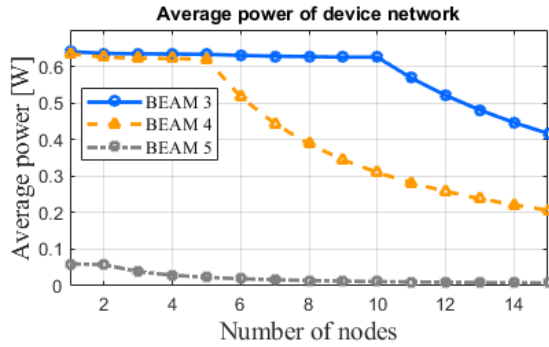


Fig. 6. Scalability analysis of the average power received of the network.

3 the efficiency drops later than with beams 4 and 5. On the contrary, higher frequencies were preferences for such type of technology, however as the results show, as the beam widens up lower frequencies are used, resulting in better efficiency results. Based on the network evaluation use of the wider beams is more beneficial as we can reach more devices with a single beam. Therefore we can recommend emphasizing beamforming research to find the most optimal beam forms and parameter configurations.

## V. CONCLUSION AND DISCUSSION

In this work, we analyse the received power and power transfer efficiency for a network of wireless neural interfaces using a proposed lateral resolution beamforming technique. We explore the beam-shape versus frequency relationship to analyse adaptable strategies based on the network configuration. Our results show that wider ultrasound beams can achieve higher distributed power conversion efficiency up to 25%. Our results show that chosen lateral resolution acoustic beamforming can be used for controlling the ultrasound beam in shape and strength. This will enable the adaptable use of ultrasound for various situations in the case of neural interfaces from individual implanted devices to the network of those devices.

## REFERENCES

[1] O. B. Akan, H. Ramezani, M. Civas, O. Cetinkaya, B. A. Bilgin, and N. A. Abbasi, "Information and communication theoretical understanding and treatment of spinal cord injuries: State-of-the-art and research challenges," *IEEE Reviews in Biomedical Engineering*, 2021.
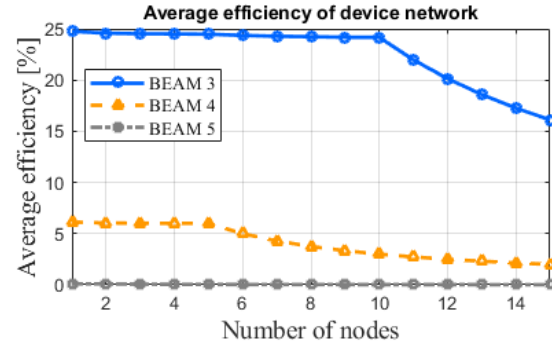
Fig. 7. Scalability analysis of the average efficiency of power transfer of network nodes.

[2] A. O. Bicen, I. F. Akyildiz, S. Balasubramaniam, and Y. Koucheryavy, "Linear channel modeling and error analysis for intra/inter-cellular ca 2+ molecular communication," *IEEE transactions on nanobioscience*, vol. 15, no. 5, pp. 488–498, 2016.

[3] B. D. Unluturk, S. Balasubramaniam, and I. F. Akyildiz, "The impact of social behavior on the attenuation and delay of bacterial nanonetworks," *IEEE transactions on nanobioscience*, vol. 15, no. 8, pp. 959–969, 2016.

[4] S. A. Wirdatmadja, S. Balasubramaniam, Y. Koucheryavy, and J. M. Jornet, "Wireless optogenetic neural dust for deep brain stimulation," in *2016 IEEE 18th International Conference on e-Health Networking, Applications and Services (Healthcom)*. IEEE, 2016, pp. 1–6.

[5] S. A. Wirdatmadja, M. T. Barros, Y. Koucheryavy, J. M. Jornet, and S. Balasubramaniam, "Wireless optogenetic nanonetworks for brain stimulation: Device model and charging protocols," *IEEE transactions on nanobioscience*, vol. 16, no. 8, pp. 859–872, 2017.

[6] D. Seo *et al.*, "Neural dust: An ultrasonic, low power solution for chronic brain-machine interfaces," *arXiv preprint arXiv:1307.2196*, 2013.

[7] L. Galluccio, T. Melodia, S. Palazzo, and G. E. Santagati, "Challenges and implications of using ultrasonic communications in intra-body area networks," in *2012 9th Annual Conference on Wireless On-Demand Network Systems and Services (WONS)*. IEEE, 2012, pp. 182–189.

[8] S. Balasubramaniam *et al.*, "Wireless communications for optogenetics-based brain stimulation: Present technology and future challenges," *IEEE Communications Magazine*, vol. 56, no. 7, pp. 218–224, 2018.

[9] B. Kohout *et al.*, "Sound field simulation tool for arbitrary rectangular transducer array matrices," in *2012 IEEE International Ultrasonics Symposium*. IEEE, 2012, pp. 568–571.

[10] D. Seo, R. M. Neely, K. Shen, U. Singhal, E. Alon, J. M. Rabaey, J. M. Carmena, and M. M. Maharbiz, "Wireless recording in the peripheral nervous system with ultrasonic neural dust," *Neuron*, vol. 91, no. 3, pp. 529–539, 2016.

[11] D. K. Piech, B. C. Johnson, K. Shen, M. M. Ghanbari, K. Y. Li, R. M. Neely, J. E. Kay, J. M. Carmena, M. M. Maharbiz, and R. Muller, "A wireless millimetre-scale implantable neural stimulator with ultrasonically powered bidirectional communication," *Nature biomedical engineering*, vol. 4, no. 2, pp. 207–222, 2020.

[12] D. Dance, S. Christofides, A. Maidment, I. McLean, and K. Ng, "Diagnostic radiology physics: A handbook for teachers and students. endorsed by: American association of physicists in medicine, asia-oceania federation of organizations for medical physics, european federation of organisations for medical physics," 2014.

[13] T. Tarnaud, W. Joseph, L. Martens, and E. Tanghe, "Computational modeling of ultrasonic subthalamic nucleus stimulation," *IEEE Transactions on Biomedical Engineering*, vol. 66, no. 4, pp. 1155–1164, 2018.

[14] I. foundation. (2021) Tissue properties - speed of sound. [Online]. Available: https://itis.swiss/virtual-population/tissue-properties/database/acoustic-properties/speed-of-sound/

[15] S. Sonmezoglu, A. Darvishian, K. Shen, M. J. Bustamante, A. Kandala, and M. M. Maharbiz, "A method and analysis to enable efficient piezoelectric transducer-based ultrasonic power and data link for miniaturized implantable medical devices," *IEEE Transactions on Ultrasonics, Ferroelectrics, and Frequency Control*, 2021.

[16] G. E. Santagati, N. Dave, and T. Melodia, "Design and performance evaluation of an implantable ultrasonic networking platform for the internet of medical things," *IEEE/ACM Transactions on Networking*, vol. 28, no. 1, pp. 29–42, 2020.